Functional Materials 12, No.1 (2005)

Phase composition and properties of Fe_2O_3–Al_2O_3 catalytic system in the high-temperature ammonia oxidation process

N.I.Zakharchenko

N.Zhukovsky National Aerospace University "KhAI",
17 Chkalov St., 61070 Kharkiv, Ukraine

Received February 25, 2004

The Fe_2O_3–Al_2O_3 catalytic system in the high-temperature ammonia oxidation reaction has been studied. The system phase composition has been shown to influence the physico-chemical properties and performance of the catalysts. The catalytic properties of the iron-aluminum system (93.3 mass % by Fe_2O_3 and 6.7 mass % by Al_2O_3) in ammonia oxidation have been determined. The causes of high-temperature catalyst deactivation have been discussed.

Исследована каталитическая система Fe_2O_3–Al_2O_3 в реакции высокотемпературного окисления аммиака. Показано влияние фазового состава системы на физико-химические и каталитические свойства катализаторов. Для катализатора состава Fe_2O_3 — 93,3 %масс., Al_2O_3 — 6,7 %масс определены оптимальные характеристики процесса окисления аммиака. Рассмотрены причины дезактивации катализатора.

The industrial nitric acid production is based on catalytic ammonia oxidation to nitric oxide using scarcely available and expensive catalysts (platinum, rhodium, and palladium alloys) [1]. The search for efficient platinum-free catalysts (PFC) is based on comprehensive studies of various compounds and composites differing in composition, structure, and chemical pre-history. It is just ammonia oxidation that is among the PFC bases of good prospects and is used in industry as a component in the second stage of combined ammonia oxidation system. Various metals are used as modifying additives to provide the high activity and selectivity of ammonia oxidation with respect to nitric oxide and to improve its thermal and chemical stability [1–5]. Among those additives, there is aluminum oxide, but the properties of Fe_2O_3–Al_2O_3 catalytic system are still not studied within a wide composition range. This work is aimed at study of the Fe_2O_3–Al_2O_3 system phase composition influence on the properties thereof in the high-temperature ammonia oxidation conditions.

The catalysts were prepared by thermal decomposing mixtures of analytical purity grade hydrated iron [$Fe(NO_3)\cdot 9H_2O$] and aluminum [$Al(NO_3)\cdot 9H_2O$] nitrate in air as described in [6]. The catalysts grains were finally heat treated at 1243 K. The X-ray phase analysis (XPA) was examined using a Siemens D-500 powder diffractometer in Cu K_α emission with a graphite monochromator in the beam to be diffracted. The IR absorption spectra were measured using a Perkin-Elmer 577 spectrophotometer in 200 to 2000 cm^{-1} range using KBr tablets as the matrices. The catalyst selectivity with respect to NO (S_{NO}) was measured according to the procedure described in [1] using an unit containing a flow type quartz reactor of 2 cm in diameter. The catalyst layer height was 4 to 12 cm, the grain size 2×3 mm^2, the ammonia content in the ammonia-air mixture

(AAM) about 10 vol. %, the contact duration $7.21 \cdot 10^{-2}$ s at normal conditions (NC), that is, the optimal value determined by experimentation, the inlet pressure 0.101 MPa. The testing temperature was 1093 K and varied within limits of 913 to 1273 K in individual sets of experiments. The reaction products of ammonia oxidation and thermal NO decomposition were analyzed according to known procedure [7] by gas chromatography, NH_3, O_2, N_2, NO, and N_2O content was determined prior to and after the mixture passage through the catalyst layer. The determination threshold (vol. p.c.) of the analysis was $3.0 \cdot 10^{-3}$ for NH_3, $3.5 \cdot 10^{-3}$ for NO, $5.0 \cdot 10^{-3}$ for O_2, N_2, and N_2O.

The catalyst limiting load with respect to ammonia N_{NH3} was determined using the procedure [2] consisting in the load increasing up to the critical "extinguishing" state, that is, up to the heat balance violation associated with the reaction regime transition from the diffusion to kinetic one. The catalyst specific surfaces were measured using the BET method (Brunauer, Emmett and Teller method) [8]. The catalyst particle size was measured using a JEM-7Y electron microscope and the procedure [9]. The reaction kinetic characteristics were determined using the "ignition" and "extinguishing" temperatures of the catalyst tablet, that is, the critical temperature points. To calculate the reaction rate, the determination method of the outer diffusion region temperature limits was employed using the catalyst tablet "extinguishing" effect at lowering AAM temperature. The catalyst surface temperature was measured by a chromel-alumel thermocouple immersed (0.3 mm depth from the upper butt) in the catalyst tablet (54 mm^2 cylinder) at the AAM income side. The incoming AAM temperature was measured by a similar thermocouple surrounded with a layer of quartz grains [10] to reduce the effect of the tablet heat emission.

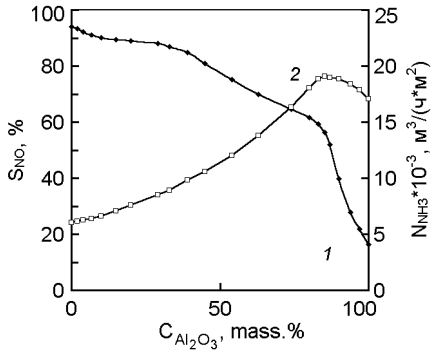

Fig. 1. Catalyst selectivity with respect to NO, S_{NO} (*1*), and limiting loading with respect to ammonia, N_{NH3} (*2*), as functions of the Fe_2O_3–Al_2O_3 system composition.

The phase composition of the studied catalyst system is presented in Table 1. The catalytic characteristics of the Fe_2O_3–Al_2O_3 system are shown in Figs. 1 and 2. Only two nitrogen compounds, N_2 and NO, were found in the ammonia oxidation products. Thus, the total ammonia conversion is 100 %. Only the N_2/NO ratio varies in the catalytic process, that is, the catalyst selectivity with respect to NO (or to nitrogen) being changed. Table 2 presents the experimental data on thermal dissociation of NO on the catalyst according to the equation

$$2NO = N_2 + O_2 . \qquad (1)$$

Table 1. Phase composition of Fe_2O_3–Al_2O_3 catalytic system at 1093 K

Al_2O_3, mass p.c.	Phase composition	Crystal structure	Lattice period, nm
0	α–Fe_2O_3	Trigonal, α–Al_2O_3 type	a = 0.5432
0–6.6	α_{ss}	Trigonal, α–Al_2O_3 type	a diminishes linearly from 0.5432 to 0.5382 as Al_2O_3 conc. rises
6.7	α_{ss} saturated	Trigonal, α–Al_2O_3 type	a = 0.5382
6.8–85.1	$\alpha_{ss} + \gamma_{ss}$	–	–
85.2	γ_{ss} saturated	Cubic, $MgAl_2O_4$	a = 0.7934
85.3–99.9	γ_{ss}	Cubic, $MgAl_2O_4$	type a increases linearly from 0.7900 to 0.7934 as Fe_2O_3 conc. rises
100.0	γ–Al_2O_3	Cubic, $MgAl_2O_4$	a = 0.7900

Notations: α_{ss}, rhombohedral structure α–Fe_2O_3 based solid solution; γ_{ss}, spinel structure γ–Al_2O_3 based solid solution.

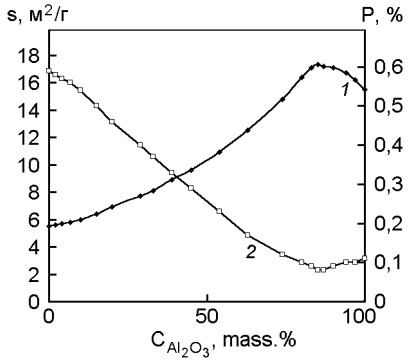

Fig. 2. Catalyst specific surface, *s* (*1*), and ammonia overshoot in critical process conditions, *P* (*2*), as functions of the Fe_2O_3–Al_2O_3 system composition.

At the selected testing temperature and optimum contact time, the NO thermal dissociation degree amounts from 1.1 % (on the low-activity composition containing 2.0 mass % Al_2O_3) to 3.5 mass % (at the Al_2O_3 content 85.2 mass %). The NO thermal dissociation results in a selectivity with respect to NO lowered by 1.0 and 2.0 mass %, respectively. The catalysts with other compositions are characterized by intermediate selectivity values (Table 2). At increased linear velocity of the reagents, that is, at the contact time shortened down to $1.2 \cdot 10^{-3}$ s (the critical conditions of the catalyst extinguishing), no thermal dissociation of NO has been observed, what is in agreement with other data on the ammonia oxidation NPC [1, 3, 4].

At the selected testing conditions, no products of chemical interaction between the components have been revealed by XPA. A similar conclusion has been made by authors [11] having studied the phase diagram of the Fe_2O_3–Al_2O_3 system. At aluminum oxide concentrations up to 6.7 mass %, rhombohedral solid solution (SS) $x\alpha$–$Fe_2O_3 \cdot y Al_2O_3$ is formed having a structure of α–Al_2O_3 type (α_{ss}). For example, the powder pattern of the catalyst containing 4.0 % by mass Al_2O_3 is characterized by main lines with interplanar distances 0.3628; 0.2693; 0.2511; 0.2214; 0.1846; 0.1695; 0.1484; 0.1454 nm typical of the α–Fe_2O_3 (hematite) rhombohedral structure [12]; those lines, however, are shifted towards larger reflection angles, thus corresponding to the lattice parameter (a) diminished from 0.5432 to 0.5402 nm. Increasing Al_2O_3 concentration in the solid solution ($C_{Al2O3} \le 6.7$ mass %) results in the (a) parameter diminution from 0.5432 to 0.5382 nm. No aluminum oxide lines are revealed in the catalyst powder pattern. Thus, within the above composition range, the catalysts are hematite based solid solutions. The Al_2O_3 solubility in α–Fe_2O_3 is limited and amounts 6.7 mass %. Increasing Al_2O_3 concentration in the rhombohedral solid solution results in a monotonous selectivity lowering (Fig. 1).

Table 2. NO decomposition extent (R_{NO}) and selectivity decrease for NO (ΔS_{NO}) on Fe_2O_3–Al_2O_3 system catalysts at 1093 K

C_{Al2O3}, %	R_{NO}, %	ΔS_{NO}, %
0 (α–Fe_2O_3)	1.1	1.0
2.0 (α_{ss})	1.1	1.0
6.7 (α_{ss} saturated)	1.2	1.1
20.0 ($\alpha_{ss} + \gamma_{ss}$)	1.4	1.2
45.0 ($\alpha_{ss} + \gamma_{ss}$)	1.9	1.5
74.0 ($\alpha_{ss} + \gamma_{ss}$)	3.0	1.9
85.2 (γ_{ss}-saturated)	3.5	2.0
94.0 (γ_{ss})	3.3	0.9
100 (γ–Al_2O_3)	3.1	0.5

Note. Gas mixture composition (vol. %): NO, 9.5; N_2, 71.3; O_2, 4.6; H_2O, 14.6. Contact time $\tau = 7.21 \cdot 10^{-2}$ s. $R_{NO} = 0$ at $\tau = 1.2 \cdot 10^{-3}$ s. Other notations as in Table 1.

In the Al_2O_3 concentration range of 85.2 to 99.9 mass %, another SS on the basis of γ–Al_2O_3 is present in the system. For example, the main powder pattern lines for a composition containing 90.0 % Al_2O_3 (0.461; 0.274; 0.2412; 0.2268; 0.1982; 0.1531; 0.1389 nm) are typical of cubic γ–Al_2O_3 based SS [12]. Increasing Fe(III) oxide concentration in that SS ($C_{Al2O3} = 85.3$ to 99.9 mass %) results in the linear increase of the (a) lattice parameter from 0.7900 to 0.7934 nm. This is explained by a partial substitution of Al^{3+} ions ($r_{Al}^{3+} = 0.057$ nm) by Fe^{3+} ones having a larger ionic radius ($r_{Fe}^{3+} = 0.067$ nm). No Fe(III) oxide lines are revealed in the catalyst powder pattern. The Fe_2O_3 solubility in γ–Al_2O_3 is limited and amounts 14.8 mass %. Increasing Al_2O_3 concentration in the cubic SS results in a sharp selectivity and specific surface lowering within the above composition range (Figs. 1, 2). The selectivity of the γ–Al_2O_3 based SS with respect to NO is much worse than that of other Fe_2O_3–Al_2O_3 system catalysts differing in composition (Fig. 1).

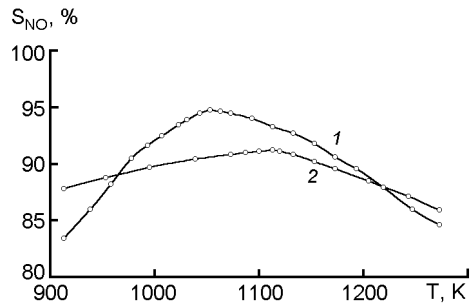

Fig. 3. Temperature dependence of selectivity, S_{NO} (p.c.) for catalysts: 93.3 % by mass Fe_2O_3 and 6.7 mass % Al_2O_3 (*1*) and α–Fe_2O_3 (2). AAM linear speed 0.18 m/s (normal conditions).

According to XPA and electron microscopy data, in the Al_2O_3 concentration range from 6.8 to 85.1 % by mass, the rhombohedral α–Fe_2O_3 based SS coexists with cubic γ–Al_2O_3 based one, both solutions forming mixtures. Increasing content of the low-selectivity γ–Al_2O_3 based SS (γ_{ss}) in the Fe_2O_3–Al_2O_3 system results in lower selectivity of the catalyst with respect to NO (Fig. 1).

The catalyst specific surface area increases from 15.5 to 17.3 m^2/g as the Fe_2O_3 content in γ–Al_2O_3 increases up to 14.8 mass %. This specific surface value exceeds the corresponding characteristics of the initial oxides. If the Fe_2O_3 content exceeds 14.8 mass %, the catalyst specific surface becomes lowered monotonously (Fig. 2). The specific surface increase in a binary system as compared to the initial oxides was observed in catalyst preparation practice [13, 14]. In [13], this phenomenon is explained by the SS lattice energy increase as compared to those if initial components. In [14], it is ascribed to the mutual protecting action occurring in the course of catalyst preparation. This action consists in adsorption of one component on the surface of crystallites of another one, resulting in the growth slowing, so the system dispersity increases. Thus, the system selectivity depends on concentrations of the SS components (Fe_2O_3 and Al_2O_3) and the ratio thereof (the Al_2O_3 content range is 6.8 to 85.1 mass %).

The limiting ammonia loading for the catalysts (Fig. 1) increases in parallel to its specific surface (Fig. 2) that is defined by the system chemical and phase composition. This is explained obviously by the corresponding increase of the number of active centers. The highest limiting loading is attained for the saturated γ–Al_2O_3 based SS (85.2 % Al_2O_3) and amounts $19.06 \cdot 10^3$ m^3 NH_3/m^2 per hour; the lowest one, for α–Fe_2O_3 ($6.06 \cdot 10^3$ m^3 NH_3/m^2 per hour). The limiting loading for γ–Al_2O_3 ($17.08 \cdot 10^3$ m^3 NH_3/m^2 per hour) is only slightly lower as compared to that for the highest activity catalyst (γ_{ss} saturated), since the specific surfaces thereof differ only slightly (Fig. 2).

In the critical process conditions (τ = $1.2 \cdot 10{-}3$ s), the consecutive reaction of NO decomposition (Eq. 1) is not observed, but some ammonia amount is found after the catalyst layer ("overshoot") (Fig. 2). As the catalyst specific surface is increased, this effect becomes weaker, what agrees well with the increased catalyst activity under critical process conditions. The maximum ammonia "overshoot" takes place for Fe_2O_3 (0.59 mass % rel.), that is, for the system having the smallest specific surface, while the minimum one, for the saturated γ–Al_2O_3 based SS (85.2 mass % Al_2O_3) (0.08 % rel.).

In the Fe_2O_3–Al_2O_3 system, the components form only solid solutions, including the two-phase SS mixtures (Table 1). The catalyst properties in such systems have been found to vary continuously from the characteristics of one component to those of the corresponding saturated SS (within the single-phase region) or from characteristics of one SS to those of the other SS (in two-phase region). Among the Fe_2O_3–Al_2O_3 system catalysts, it is just the compositions containing up to 20 % by mass of Al_2O_3 that are of a practical interest, since those show a sufficiently high selectivity (S_{NO} = 88.9 to 94.0 %). Other catalysts, including γ–Al_2O_3, exhibit rather low selectivity (Fig. 1). The Fe_2O_3 losses its selectivity rather fast in the course of service at elevated temperatures [6], that is it is unstable. We have considered the effect of Al_2O_3 additive on the phase composition and selectivity of the modified catalyst under operating conditions taking a Fe_2O_3–Al_2O_3 system containing 6.7 mass % Al_2O_3. This catalyst exhibits a rather high activity and selectivity with respect to NO (Fig. 1) and was not studied before. The temperature dependence of the catalyst selectivity is shown in Fig. 3. The selectivity maximum (91.2 %) is shifted towards higher temperatures as compared to α–Fe_2O_3 (1113 and 1053 K, respectively). The selectivity change in the 913 to 1273 K range is less sharp as com-

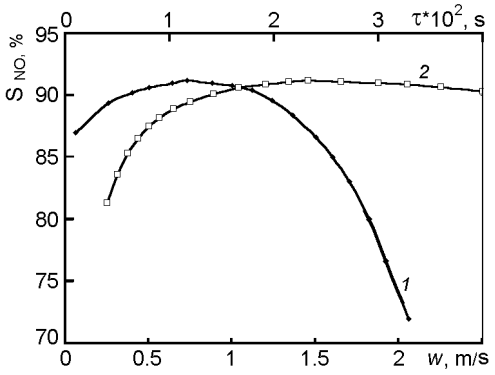

Fig. 4. Catalyst (93.3 % by mass Fe_2O_3 and 6.7 mass % Al_2O_3) selectivity dependence on AAM linear speed (w, m/s) at $\tau = 2.33 \cdot 10^{-2}$ s (service conditions) (*1*) and contact time (τ, s; service conditions) at $w = 0.73$ m/s (*2*). $T = 1113$ K.

pared to iron oxide catalyst. At $T > 1227$ K, the Fe–Al catalyst selectivity exceeds that of the iron oxide one (Fig. 3).

The dependence of the catalyst selectivity on the contact time is shown in Fig. 4. At the contact time $\tau < 1.0 \cdot 10^{-2}$ s, the sharp selectivity lowering is associated with the side reaction of nitrogen neutralization [15]:

$$4NH_3 + 6NO = 5N_2 + 6H_2O. \quad (2)$$

At $\tau > 3.2 \cdot 10^{-2}$ s, the selectivity decreases slowly, mainly due to NO dissociation (1) [1]. The optimum contact time for the catalyst is $7.21 \cdot 10^{-2}$ s under normal conditions ($2.33 \cdot 10^{-2}$ s under operating conditions). The reagent linear speed effect on the catalyst selectivity (Fig. 4) evidences the macro-kinetic process region [2–4] when the reaction rate is limited by the ammonia diffusion from the flow core to the catalyst surface. The optimum AAM linear speed is 0.73 m/s under operating conditions (0.18 m/s under operating conditions). The increase of the reagent linear speed is accompanied by the "hot zone" toward the catalyst layer outlet, that is, it results in the temperature fall of its inlet layer [1, 4]. So at $w = 2.20$ m/s, the inlet layer temperature drops down to 879 K, thus favoring the side reactions, in particular, the nitrogen neutralization rate (2) is close to maximum at that temperature [16]. Besides, the inlet layer low temperature favors the parallel process

$$4NH_3 + 3O_2 = 2N_2 + 6H_2O \quad (3)$$

resulting in the catalyst selectivity lowering with respect to NO. The low AAM linear speed values, according to (3, 4), favor the side reaction of NO dissociation, thus causing a slow lowering of the catalyst selectivity, since the NO decomposition rate is rather low at $T = 1113$ K [1, 16]. The reagent linear speed increase up to critical values ($\tau = 1.2 \cdot 10^{-3}$ s) results in a distortion of the process heat balance due to a sharp increase of heat losses.

The process kinetic parameters have been calculated using the equation proposed by Buben [17] and solved for two reaction rate values at a constant oxygen concentration. The Buben equation has the form

$$(1 + a)^2[1 + (m - 1)\frac{a}{b}] - \frac{a}{\varepsilon}(1 - \frac{a}{b}) = 0, \quad (4)$$

$$a = \frac{T}{T_0} - 1, \quad b = \frac{Q\beta C_0}{\alpha T_0}, \quad \varepsilon = \frac{RT_0}{E},$$

where m is the reaction order with respect to ammonia; T, the catalyst surface temperature in the critical point; T_0, the AAM temperature; C_0, the ammonia concentration in the flow; α and β, the mass transfer and heat transfer coefficients, respectively; Q, the reaction thermal effect; E, the reaction activation energy. The α and β values were calculated using the known equations [18]. The following values have been obtained: the catalyst ignition temperature 618 K; ammonia concentration in the AAM, 10 % by vol.; the reaction activation energy $E = 38.74$ kJ/mole NH_3; the reaction order with respect to ammonia, 0.35. These values agree well with similar data for other ammonia oxidation NPC [1, 19]. In particular, for the Co_3O_4 catalyst, the activation energy amounts 37.71 kJ/mole NH_3.

The studied dependences of the catalyst selectivity on the operating time (Fig. 5) evidence a higher stability of the Fe_2O_3–Al_2O_3 catalyst as compared to α–Fe_2O_3. At optimum temperature 1113 K, the catalyst selectivity falls by 1.1 % after 102 h service. In the same testing conditions, the iron oxide selectivity drops by 2.7 %. As the process temperature rises, the catalyst deactivation becomes intensified. So at 1243 C, the selectivity drop for the Fe_2O_3–Al_2O_3 catalyst and α–Fe_2O_3 one amounted 2.3 and 9.7 % (see Fig. 5). The XRD patterns of the Fe_2O_3–Al_2O_3 catalyst after operation at 1243 K contain both lines of rhombohedral

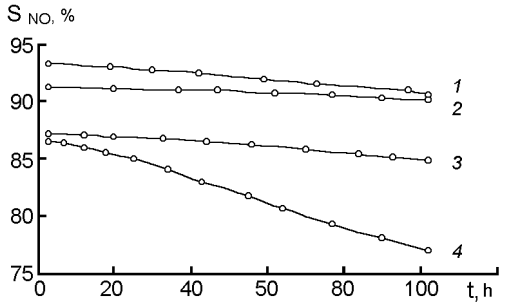

Fig. 5. Selectivity with respect to NO as a function of service time (*h*) for catalysts: α–Fe_2O_3, 1113 K (1); Fe_2O_3 — 6.7 mass % Al_2O_3 1113 K (*2*); Fe_2O_3 — 6.7 mass % Al_2O_3 1243 K (*3*); α–Fe_2O_3, 1243 K (*4*).

SS of Al_2O_3 in hematite as well as weak lines with interplanar distances 0.476; 0.291; 0.2481; 0.2052; 0.1581; 0.1456; 0.1074 nm typical of $FeAl_2O_4$ spinel (hercynite) [12]. The hercynite and Fe_2O_3–Al_2O_3 catalyst do not form solid solutions but a mixture of individual phases. The hercynite formation is confirmed by IR spectroscopy. The IR spectra of the used catalyst surface layers include the absorption bands at 500, 565, 710, 1040, 1660 cm^{-1} typical of $Fe_2Al_2O_4$ [20]. The catalyst heat treated at 1243 K in air does not show the phase transformations with $FeAl_2O_4$ formation, that is, it is thermally stable under those conditions. Therefore, the catalyst phase transformations during the high-temperature ammonia oxidation are associated with the effect of the redox reaction medium and the redox mechanism of the reaction running [3, 4, 21]. The $FeAl_2O_4$ formation is explained by the high-temperature interaction of aluminum oxide present in the catalyst with magnetite (Fe_3O_4) being a product of iron oxide phase transformation [6] according to reaction

$$Fe_3O_4 + Al_2O_3 = FeAl_2O_4 + Fe_2O_3. \quad (5)$$

The magnetite may arise both due to the redox mechanism of ammonium oxidation [3, 4, 21] and due to direct interaction of the catalyst surface areas where the catalyst-to-oxygen bond energy is low with a strong reducing agent (ammonia):

$$9(Fe_xAl_{1-x})_2O_3 + 2xNH_3 = 6xFe_3O_4 + \quad (6)$$
$$+ 9(1 - x)Al_2O_3 + xN_2 + 3xH_2O.$$

In fact, the EPR spectra of the used catalyst surface layers contain broad bands typical of ferromagnetic compounds and identical to magnetite spectrum. The magnetite formation is confirmed by IR spectroscopy. The IR spectra of the magnetic fractions from used catalyst surface layers include the absorption bands at 407, 427, 481, 673, 980 cm^{-1} typical of Fe_3O_4 [20]. The major amount of the magnetite formed is bound chemically in $FeAl_2O_4$ revealed in experiments. The magnetite as an intermediate of the catalyst phase transformations suppresses the selectivity, being a low-activity component [6] (S_{NO} = 7.0 % at 1073 K). The Fe^{3+} ion deficiency in the catalyst surface layer due to magnetite formation results in an increased Al_2O_3 concentration, that is, a local decomposition of the saturated Al_2O_3 SS in hematite, the Al_2O_3 becomes precipitated as a separate phase.

Aluminum oxide is thermodynamically stable under high-temperature (1073 to 1273 K) exposure to ammonia [22], that is, it is not reduced to the metal but exists as an individual phase at the catalyst surface and is one of initial reagents in the $FeAl_2O_4$ formation reaction (5). The surface layer XPA results of the catalyst used at 1243 K (after the magnetic fraction is removed) show that the cubic γ–Al_2O_3 is transformed into rhombohedral α–Al_2O_3 at that temperature (the main XRD lines 0.3479; 0.2552; 0.2379; 0.2084; 0.1740; 0.1602; 0.1425; 0.1374; 0.1238 nm), although literature sources point that these phase transformations occur at $T \geq 1373$ K [23]. According to data from [22, 23], Fe_2O_3 addition, even in microamounts, results in a lowered temperature of the γ–$Al_2O_3 \rightarrow$ α–Al_2O_3 phase transition. In mechanical mixture identical to the catalyst in composition (α–Fe_2O_3 93.3 %, γ–Al_2O_3 6.7 mass %) where the component interaction is restricted, a similar γ–$Al_2O_3 \rightarrow \alpha Al_2O_3$ phase transition was revealed after heat treatment at 1243 K. In particular, in the IR spectra of the mechanical mixture, the bands typical of γ–Al_2O_3 (433, 550, 610, 634, 780, 810, 850, 900 cm^{-1}) disappear after the heat treatment and those of α–Al_2O_3 appear (450, 490, 602, 642, 760 cm^{-1}). The α–Al_2O_3 absorption bands were found in the IR spectra of the used catalyst surface layers. As to the phase composition of the used catalyst subsurface layers, in the initial rhombohedral hematite-based SS, γ–Al_2O_3 is transformed into α–Al_2O_3, the rhombohedral SS structure being conserved.

The γ–Al_2O_3 selectivity is 4.5 % at 1093 K and 0.5 % at 1243 K, that is, lower

than that of γ–Al_2O_3 (Fig. 1). The selectivity of iron aluminate ($FeAl_2O_4$) synthesized as described in [24] was 6.9 and 2.4 % at 1093 and 1243 K, respectively. Thus, hercynite (Fe_3O_4) as well as both α- and γ-modifications of Al_2O_3 suppresses the iron-aluminum oxide catalyst. After 102 h service at 1243 K, the catalyst contained 2.0 % by mass of $FeAl_2O_4$. In surface layers of an iron oxide catalyst tested in the same conditions, the Fe_3O_4 concentration amounted 11.8 mass %. The phase transition intensity in the SS catalyst $(Fe_xAl_{1-x})_2O_3$ is considerably lower than that of individual Fe(III) oxide. Thus, aluminum oxide addition slows the magnetite formation and favors the retaining of catalyst selectivity (Fig. 5). Thermodynamic probability of magnetite formation (Eq.(6)) is increased with temperature elevation, similar to transformation of Fe(III) oxide [25] according to the scheme

$$9Fe_2O_3 + 2NH_3 = 6Fe_3O_4 + N_2 + 3H_2O. \quad (7)$$

Thermodynamic probability of $FeAl_2O_4$ oxidation (as well as that of magnetite) with oxygen contained in AAM according to the equation

$$4FeAl_2O_4 + O_2 = 2Fe_2O_3 + 4Al_2O_3 \quad (8)$$

is lower than that of processes (5) and (6) and becomes lower as the reaction temperature rises [25, 26]. Thus, the above compounds tend to be accumulated in the catalyst surface layer at elevated temperatures. The Fe(III) oxide formed due to reactions (5) and (8) is subjected to intense phase transformations (Eq.(7)) resulting in magnetite [6] that, in turn, is involved in the formation of the low-selectivity $FeAl_2O_4$. The hematite interaction with Al(III) oxide at the catalyst surface (SS formation) at 1243 K is hindered [26]. The high-temperature redox processes of new phase (Fe_3O_4, $FeAl_2O_4$, Al_2O_3) formation and the catalyst surface recovery are unbalanced and shifted towards the accumulation of low-selectivity $FeAl_2O_4$, as has been revealed in experiments. The phase transformation unbalance is increased as the temperature rises.

Moreover, under elevated temperature, the catalyst is subjected to recrystallization with the specific surface area reduction from 5.2 to 2.9 m^2/g (Table 3) after 102 h at 1243 K and thus, the number of active centers at the surface is diminished [1]. The catalyst particle linear dimension is increased from 80 to 250 nm. Since the reaction runs in subcritical conditions, i.e., it is limited by ammonia diffusion to the catalyst outer surface, the specific surface value is not critical for the catalyst selectivity with respect to NO [1–4]. That is, the selectivity drop at 1243 K is due mainly to phase and chemical transformations of the catalyst. In critical conditions (the catalyst "extinguishing"), the recrystallization and specific surface reduction cause a lowering of the catalyst limiting loading from $5.73 \cdot 10^3$ to $3.19 \cdot 10^3$ m^3 NH_3/m^2 per hour (102 h service).

Thus, the high-temperature deactivation of Fe–Al oxide catalyst is due to a combination of chemical and phase transformations resulting in low-activity and low-selectivity components (Fe_3O_4, $FeAl_2O_4$, Al_2O_3) and

Table 3. Changes in structure and catalytic properties of Fe–Al catalyst (Al_2O_3 6.7 mass %) during service at 1243 K

t, h	S_{NO}, %	s, m^2/g	n, nm	$N \cdot 10^{-3}$ $m^3/(h \cdot m^2)$
3	87.1	5.2	80	5.73
12	87.0	5.0	92	5.51
20	86.9	4.7	102	5.18
33	86.7	4.4	123	4.85
44	86.5	4.1	143	4.52
56	86.2	3.8	170	4.19
70	85.8	3.5	199	3.86
84	85.4	3.2	223	3.53
93	85.1	3.1	237	3.42
102	84.8	2.9	250	3.19

Notations: t, service duration; n, r.m.s. particle size.

structure changes (recrystallization and specific surface reduction).

To conclude, the phase composition and physicochemical properties of Fe_2O_3–Al_2O_3 catalytic system in the high-temperature ammonia oxidation reaction have been studied. The physicochemical properties and catalytic efficiency of the system have been found to depend on the phase and chemical composition of α–Fe_2O_3 and γ–Al_2O_3 solid solutions and the quantitative ratio between the solid solutions. For the catalyst containing 93.3 mass % Fe_2O_3 and 6.7 mass % Al_2O_3, optimum conditions of ammonia oxidation process have been found as follows: temperature 1113 K, contact time $7.21 \cdot 10^{-2}$ s, the reagent linear speed 0.18 m/s, activation energy 38.74 kJ/mole NH_3. At 1113–1243 K, the catalyst tends to deactivation caused by chemical and phase transformations resulting in low-activity and low-selectivity components (Fe_3O_4, $FeAl_2O_4$, Al_2O_3) in combination with structure changes (recrystallization and specific surface reduction).

References

1. M.M.Karavaev, A.P.Zasorin, N.F.Kleschev, Catalytic Oxidation of Ammonia, Khimia, Moscow (1983) [in Russian].
2. N.M.Morozov, L.I.Lukyanova, M.I.Temkin, *Kinetika i Kataliz*, **7**, 172 (1966).
3. N.I.Zakharchenko, V.V.Seredenko, *Zh. Prakt. Khim.*, **72**, 1921 (1999).
4. N.I.Zakharchenko, *Zh. Fiz. Khim.*, **75**, 985 (2001).
5. N.I.Zakharchenko, *Functional Materials*, **8**, 339 (2001).
6. A.P.Zasorin, N.I.Zakharchenko, M.M.Karavaev, *Izv. VUZov, Khim. Khim. Tekhnol.*, **23**, 1274 (1980).
7. T.G.Alkhazov, G.Z.Gassan-Zade, M.O.Osmanov, M.Yu.Sultanov, *Kinetika i Kataliz*, **16**, 1230 (1975).
8. N.E.Buyanova, A.P.Karnaukhov, Yu.A.Alabuzhev, Determination of Specific Surface of Catalysts, Khimia, Moscow (1973) [in Russian].
9. V.M.Lukyanovich, Electron Microscopy in Physicochemical Studies, AN SSSR Publ., Moscow (1960) [in Russian].
10. V.S.Beskov, M.M.Karavaev, D.V.Garov, V.A.Arutyunyan, *Reaction Kinet. and Catal. Lett.*, **4**, 351 (1976).
11. A.Muan, *Am. J. Sci.*, **6**, 413 (1958).
12. Powder diffraction data file. ASTM, Joint Committee in Powder Diffraction Standards. Philadelphia (1967), p.347.
13. A.L.Klyachko-Gurvich, A.M.Rubinshtein, in book: Kinetics and Catalysis Problems: Scientific Principles of Catalyst Selection for Heterogeneous Chemical Reactions, Nauka, Moscow (1966), p.41 [in Russian].
14. W.O.Milligan, C.R.Adams, *J. Phys. Chem.*, **57**, 885 (1953).
15. S.N.Ganz, A.M.Vashkevich, *Zh. Prakt. Khim.*, **43**, 13 (1970).
16. B.A.Zhidkov, S.S.Orlova, G.A.Bochenko, A.S.Plygunov, *Khim. Tekhnol.*, **1**, 5 (1979).
17. N.Ya.Buben, *Zh. Fiz. Khim.*, **19**, 250 (1945).
18. A.G.Kasatkin, Basic Processes and Apparatus of Chemical Technology, Khimia, Moscow (1973) [in Russian].
19. F.S.Shub, L.O.Apelbaum, M.I.Temkin, in: Proc. of 2nd All-Union Conf. on Kinetics of Catalytic Reactions, Inst. for Catalysis Publ., Siber. Div. AN SSSR, Novosibirsk, 1, 13 (1975) [in Russian].
20. K.Lowson, Infrared Absorption of Inorganic Substances. Reinhold Publishing Corporation, New-York (1961).
21. G.I.Golodetz, Heterogeneous Catalytic Reactions Involving Molecular Oxygen, Naukova Dumka, Kiev (1977) [in Russian].
22. Physical and-Chemical Aspects of Adsorbents and Catalysts. Ed. by B.G.Linsen. Academic Press, London, (1970).
23. H.P.Rooksby, The X-Ray Identification and Crystal Structures of Clay Minerals. Mineral. Soc., London (1961), p.457.
24. A.Hoffman, W.A.Fischer, *Z. Anorg. Chem.*, **7**, 80 (1956).
25. N.I.Zakharchenko, I.N.Protiven', NIITEKHIM, Cherkassy, Depos. No.128-KhP-93 (1993) [in Russian].
26. Yu.D.Tretyakov, Solid Phase Reactions, Khimia, Moscow (1978) [in Russian].

Фазовий склад і властивості каталітичної системи Fe_2O_3–Al_2O_3 в процесі високотемпературного окислення аміаку

М.І.Захарченко

Досліджено каталітичну систему Fe_2O_3–Al_2O_3 в реакції високотемпературного окислення аміаку. Показано вплив фазового складу системи на фізико-хімічні і каталітичні властивості каталізаторів. Визначені каталітичні властивості залізо-алюмінійового каталізатора (Fe_2O_3 — 93,3 мас.%, Al_2O_3 — 6,7 мас.%) окислення аміаку. Розглянуто причини високотемпературної дезактивації каталізатора.